Supplement of

Fast online characterization of novel VOC permeation tubes by TD-GC-FID: Direct quantification via the effective carbon number concept

Ali Ghaddar[1,2], Mathilde Mascles[2], Jean-Philippe Amiet[2], Damien Bazin[2], Stéphane Le Calvé[1]
[1]Institute for Chemistry and Processes for Energy, the Environment and Health (ICPEES), UMR 7515, CNRS/University of Strasbourg, Strasbourg, 67087, France.
[2]Chromatotec, Saint-André-de-Cubzac, 33240, France.

Correspondence to: Stéphane Le Calvé (slecalve@unistra.fr)

Table S1. Chemical family and physical properties of the investigated compounds in this work.

VOC_i (CAS n°)	Chemical family	Properties
Benzene **(71-43-2)**	Aromatic	MW[a] (g/mol): 78.11 MP[b] (°C): 5.5 BP[c] (°C): 80.08 VP[d] (mmHg): 94.8 d[e] (g/cm^3): 0.879
***(E)*-2-hexenal** **(6728-26-3)**	Aldehyde	MW[a] (g/mol): 98.14 MP[b] (°C): –78 (estimate) BP[c] (°C): 146.5 VP[d] (mmHg): 4.11 d[e] (g/cm^3):0.8491
2-methyl-1-butanol **(78-92-2)**	Alcohol	MW[a] (g/mol): 88.15 MP[b] (°C): –117.2 BP[c] (°C): 127.5 VP[d] (mmHg): 3.13 d[e] (g/cm^3): 0.8152
D-limonene **(5989-27-5)**	Monoterpene	MW[a] (g/mol): 136.23 MP[b] (°C): –74 BP[c] (°C): 177.6 VP[d] (mmHg): 2.33 d[e] (g/cm^3): 0.841

[a]molecular weight, [b]melting point, [c]boiling point, [d]vapor pressure at 25 °C, [e]density at 20 °C.

Table S2. Effective carbon numbers (ECN) and relative response factors (RF) for the investigated compounds calculated relative to the response factor of the reference compound for TD-GC-FID calibration, i.e., benzene. ECN reduction factor data were retrieved from Sternberg et al. (1962).

VOC_i	Carbon number	Theoretical ECN_{VOC_i}	ECN_{VOC_i} reduction factor	RF_{VOC_i}
Benzene	6	6	0	1 (RF_{ref})
***(E)*-2-hexenal**	6	4.95	–1 (carbonyl) –0.05 (olefinic)	1.52
2-methyl-1-butanol	5	4.4	–0.05 (olefinic)	1.54
D-limonene	10	9.85	–0.05 (olefinic)	1.12

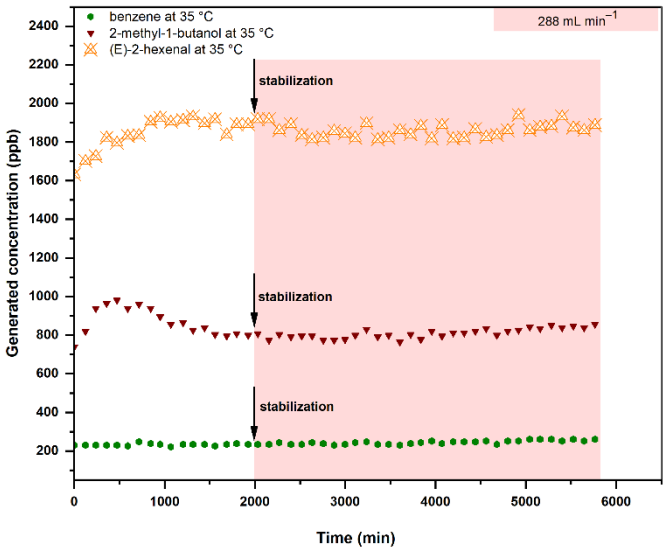

Figure S1. Time profiles of the generated concentrations at a total flow rate of 288 mL min^{-1} and their stabilization after a window of 2000 min (≈1.4 days) for three target VOCs at 35 °C (benzene, *(E)*-2-hexenal, and 2-methyl-1-butanol) during repeated TD-GC-FID cycles over several days.

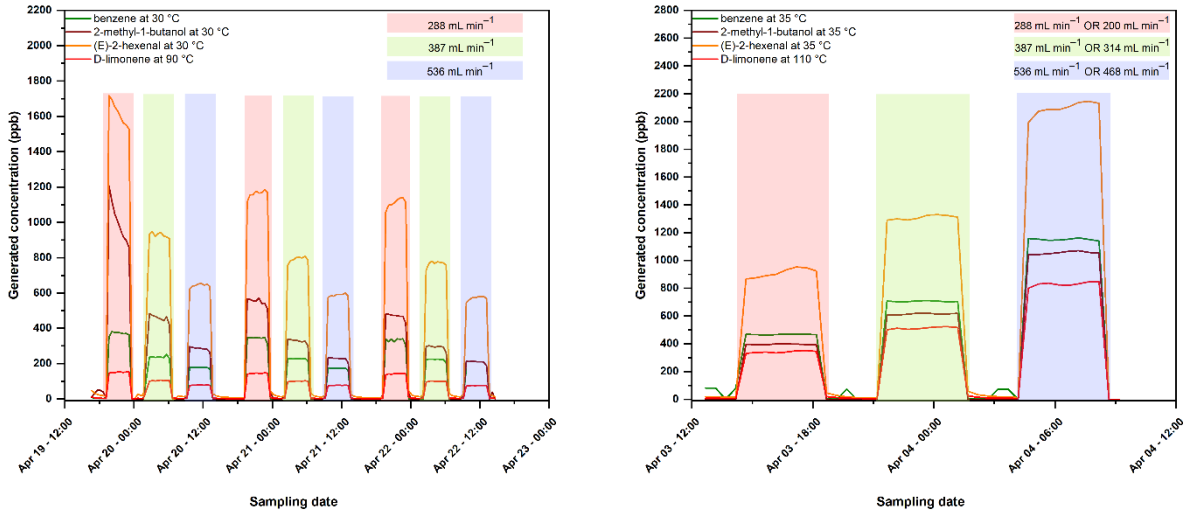

(a) **(b)**

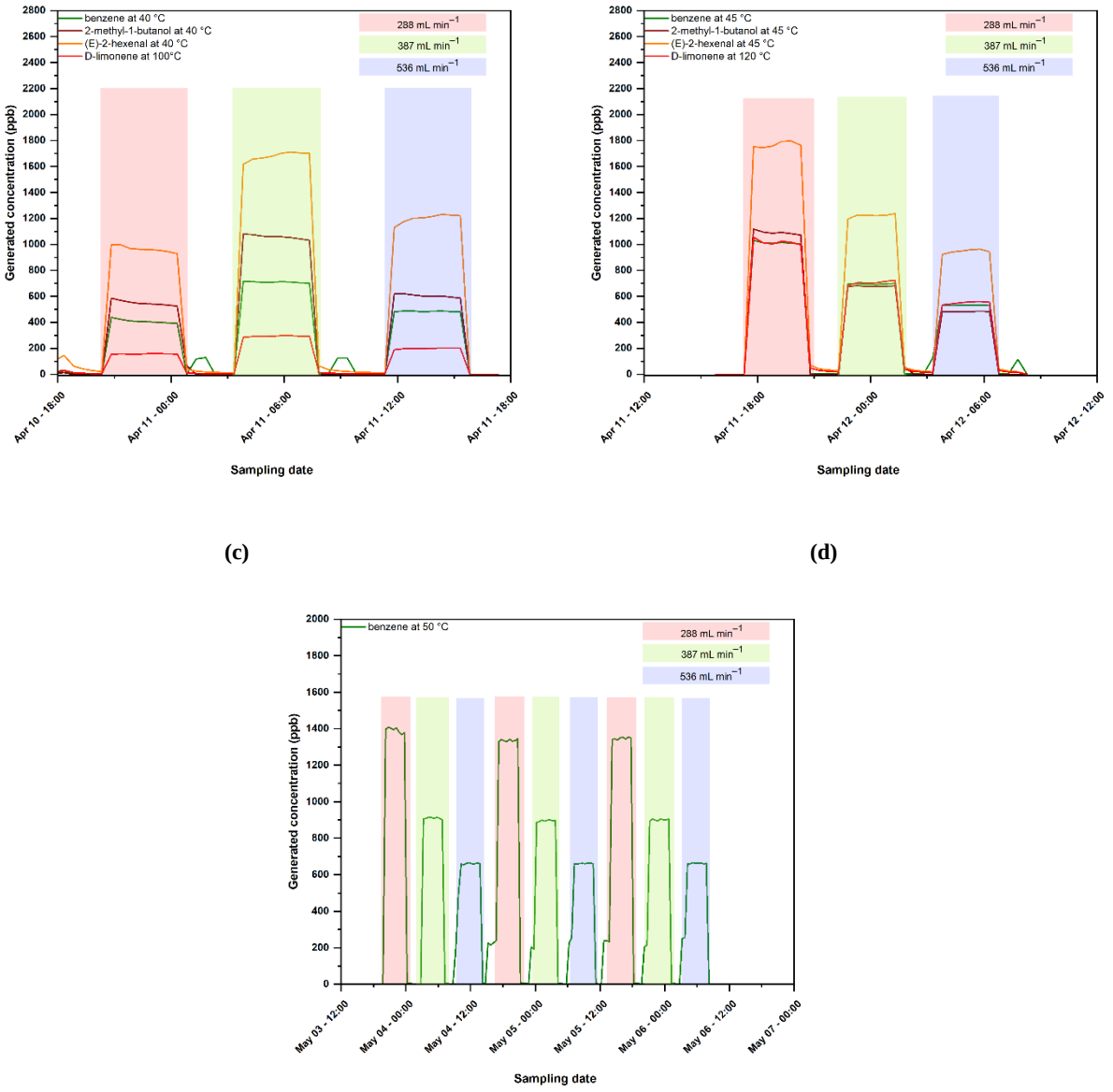

Figure S2. Temporal evolution of the generated concentrations at different total flow rates and different permeation oven temperatures of **a)** 30 °C for benzene, 2-methyl-1-butanol, and *(E)*-2-hexenal and 90 °C for D-limonene, **b)** 35 °C for benzene, 2-methyl-1-butanol, and *(E)*-2-hexenal and 110 °C for D-limonene, **c)** 40 °C for benzene, 2-methyl-1-butanol, and *(E)*-2-hexenal and 100 °C for D-limonene, **d)** 45 °C for benzene, 2-methyl-1-butanol, and *(E)*-2-hexenal and 120 °C for D-limonene, and **e)** 50 °C for benzene. Reproducibility in terms of replicates of each total flow rate differs from one temperature to another ($n_{(a)}$, $n_{(e)} = 3$, $n_{(b)}$, $n_{(c)}$, $n_{(d)} = 1$). Shaded areas correspond to the total dilution flow rates of dry zero-air controlled by the three mass flow controllers (rounded values for clarity: red for 288- or 200-mL min^{-1}, light green for 387- or 314-mL min^{-1}, and blue for 536- or 468-mL min^{-1}). Blank measurements ($n \geq 4$) were acquired between continuous measurements of the generated gas mixture from the permeation ovens (n = 8).

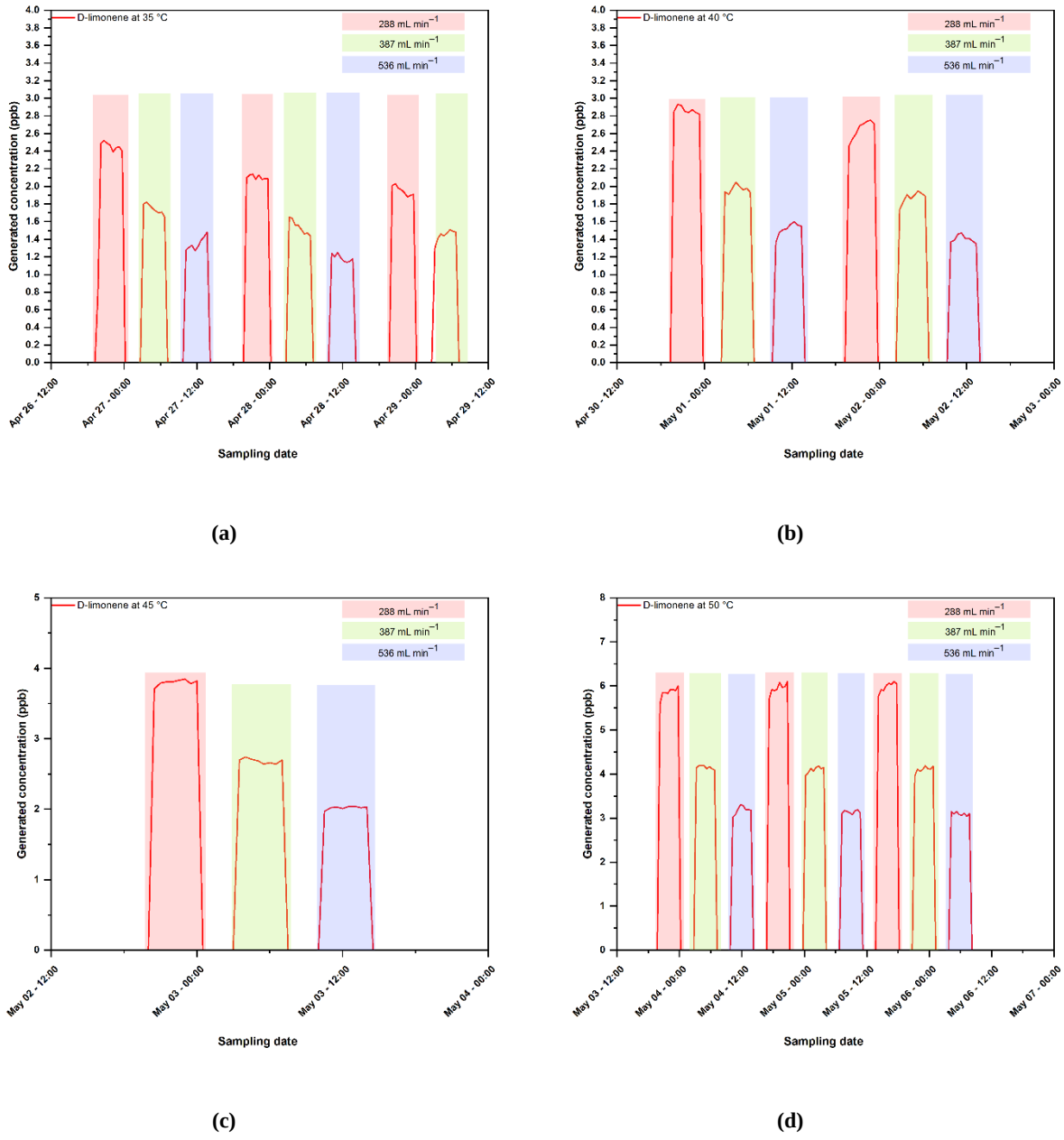

Figure S3. Temporal evolution of the generated concentrations of D-limonene at different total flow rates and permeation oven temperatures of **a)** 35 °C, **b)** 40 °C, **c)** 45 °C, and **d)** 50 °C. Reproducibility in terms of replicates of each total flow rate differs from one temperature to another ($n_{(a)}$, $n_{(d)} = 3$, $n_{(b)} = 2$, $n_{(c)} = 1$). Shaded areas correspond to the total dilution flow rates of dry zero-air controlled by the three mass flow controllers (rounded values for clarity: red for 288- or 200-mL min^{-1}, light green for 387- or 314-mL min^{-1}, and blue for 536- or 468-mL min^{-1}). Blank measurements ($n \geq 4$) were acquired between continuous measurements of the generated gaseous D-limonene from the permeation oven (n = 8).

Table S3. Average generated concentrations of benzene at the investigated permeation oven temperatures (25, 30, 35, 40, 45, and 50 °C) and total dilution flow rates of MFC1, MFC2, and MFC3 (288.2-, 387.0-, and 536.4-mL min^{-1}). The table reports the mean concentration, relative standard deviation (RSD), and the total number of measurements for each operating condition (n_{total}). The reported n_{total} includes all the measurements acquired over multiple experimental days (intermediate precision).

Flow	**288.2**			**387.0**			**536.4**		
Temperature (°C)	[benzene] (ppb)	RSD	n_{total}	[benzene] (ppb)	RSD	n_{total}	[benzene] (ppb)	RSD	n_{total}
25	353.7	0.7%	24	226.7	4.7%	24	149.9	3.9%	24
30	347.8	5.8%	24	228.5	3.4%	24	172.9	2.3%	24
35	562.5	5.6%	24	362.6	8.9%	24	271.6	13.5%	24
40	1013.7	2.9%	16	668.7	1.7%	16	486.6	1.5%	16
45	1047.4	4.6%	16	706.2	2.0%	16	526.2	1.3%	16
50	1358.3	2.2%	24	902.1	0.8%	24	661.6	0.1%	24

Table S4. Average generated concentrations of *(E)*-2-hexenal **(a)** at the investigated permeation oven temperatures (25, 30, and 40 °C) and total dilution flow rates of MFC1, MFC2, and MFC3 (288.2-, 387.0-, and 536.4-mL min^{-1}); and **(b)** at 35 °C and total dilution flow rates of MFC1, MFC2, and MFC3 (200.0-, 314.0-, and 468.5-mL min^{-1}). The table reports the mean concentration, relative standard deviation (RSD), and the total number of measurements for each operating condition (n_{total}). The reported n_{total} includes all the measurements acquired over multiple experimental days (intermediate precision).

Flow	**288.2**			**387.0**			**536.4**		
Temperature (°C)	[*(E)*-2-hexenal] (ppb)	RSD	n_{total}	[*(E)*-2-hexenal] (ppb)	RSD	n_{total}	[*(E)*-2-hexenal] (ppb)	RSD	n_{total}
25	1000.9	6.2%	24	675.6	5.9%	24	495.8	5.3%	24
30	1296.3	21.5%	24	828.02	10.6%	24	599.9	6.32%	24
40	1723.5	3.6%	16	1211.0	1.2%	16	955.5	1.3%	16

(a)

Flow	**200.0**			**314.0**			**468.5**		
Temperature (°C)	[*(E)*-2-hexenal] (ppb)	RSD	n_{total}	[*(E)*-2-hexenal] (ppb)	RSD	n_{total}	[*(E)*-2-hexenal] (ppb)	RSD	n_{total}
35	2134.1	2.6%	16	1308.8	1.2%	8	910.5	3.6%	8

(b)

Table S5. Average generated concentrations of 2-methyl-1-butanol **(a)** at the investigated permeation oven temperatures (25, 30, 40, and 45 °C) and total dilution flow rates of MFC1, MFC2, and MFC3 (288.2-, 387.0-, and 536.4-mL min^{-1}); and **(b)** at 35 °C and total dilution flow rates of MFC1, MFC2, and MFC3 (200.0-, 314.0-, and 468.5-mL min^{-1}). The table reports the mean concentration, relative standard deviation (RSD), and the total number of measurements for each operating condition (n_{total}). The reported n_{total} includes all the measurements acquired over multiple experimental days (intermediate precision).

Flow	**288.2**			**387.0**			**536.4**		
Temperature (°C)	[2-methyl-1-butanol] (ppb)	RSD	n_{total}	[2-methyl-1-butanol] (ppb)	RSD	n_{total}	[2-methyl-1-butanol] (ppb)	RSD	n_{total}
25	381.1	16.1%	24	227.7	9.5%	24	158.4	6.7%	24
30	673.3	42.7%	24	359.3	24.3%	24	240.4	16.6%	24
40	1058.1	1.4%	8	607.0	1.9%	8	549.1	3.6%	8
45	1091.4	1.4%	8	678.2	0.4%	8	482.7	0.3%	8

(a)

Flow	**200.0**			**314.0**			**468.5**		
Temperature (°C)	[2-methyl-1-butanol] (ppb)	RSD	n_{total}	[2-methyl-1-butanol] (ppb)	RSD	n_{total}	[2-methyl-1-butanol] (ppb)	RSD	n_{total}
35	1064.8	1.4%	16	614.4	0.9%	8	396.7	0.3%	8

(b)

Table S6. Average generated concentrations of D-limonene **(a)** at the investigated permeation oven temperatures (35, 40, 45, 50, 80, 90, 100, and 120 °C) and total dilution flow rates of MFC1, MFC2, and MFC3 (288.2-, 387.0-, and 536.4-mL min^{-1}); and **(b)** at 90 and 110 °C and total dilution flow rates of MFC1, MFC2, and MFC3 (200.0-, 314.0-, and 468.5-mL min^{-1}). The table reports the mean concentration, relative standard deviation (RSD), and the total number of measurements for each operating condition (n_{total}). The reported n_{total} includes all the measurements acquired over multiple experimental days (intermediate precision).

Flow	**288.2**			**387.0**			**536.4**		
Temperature (°C)	[D-limonene] (ppb)	RSD	n_{total}	[D-limonene] (ppb)	RSD	n_{total}	[D-limonene] (ppb)	RSD	n_{total}
35	2.07	13.94%	32	1.52	11.31%	32	1.19	12.61%	24
40	2.76	5.51%	16	1.92	3.45%	16	1.46	5.56%	16
45	3.80	1.12%	8	2.69	1.32%	8	2.02	1.12%	8
50	5.93	1.07%	24	4.12	0.70%	24	3.14	1.33%	24
80	79.0	4.10%	24	54.2	2.52%	24	41.0	2.96%	24
90	145.9	3.04%	24	101.1	2.25%	24	76.9	1.61%	24
100	292.6	1.49%	8	198.9	2.05%	8	156.9	0.95%	8
120	1018.1	2.03%	8	706.1	1.99%	8	550.2	1.82%	8

(a)

Flow	**200.0**			**314.0**			**468.5**		
Temperature (°C)	[D-limonene] (ppb)	RSD	n_{total}	[D-limonene] (ppb)	RSD	n_{total}	[D-limonene] (ppb)	RSD	n_{total}
90	n.a.	n.a.	n.a.	139.1	2.12%	8	97.6	1.28%	8
110	829.5	1.80%	8	512.7	1.55%	8	341.2	2.14%	8

(b)

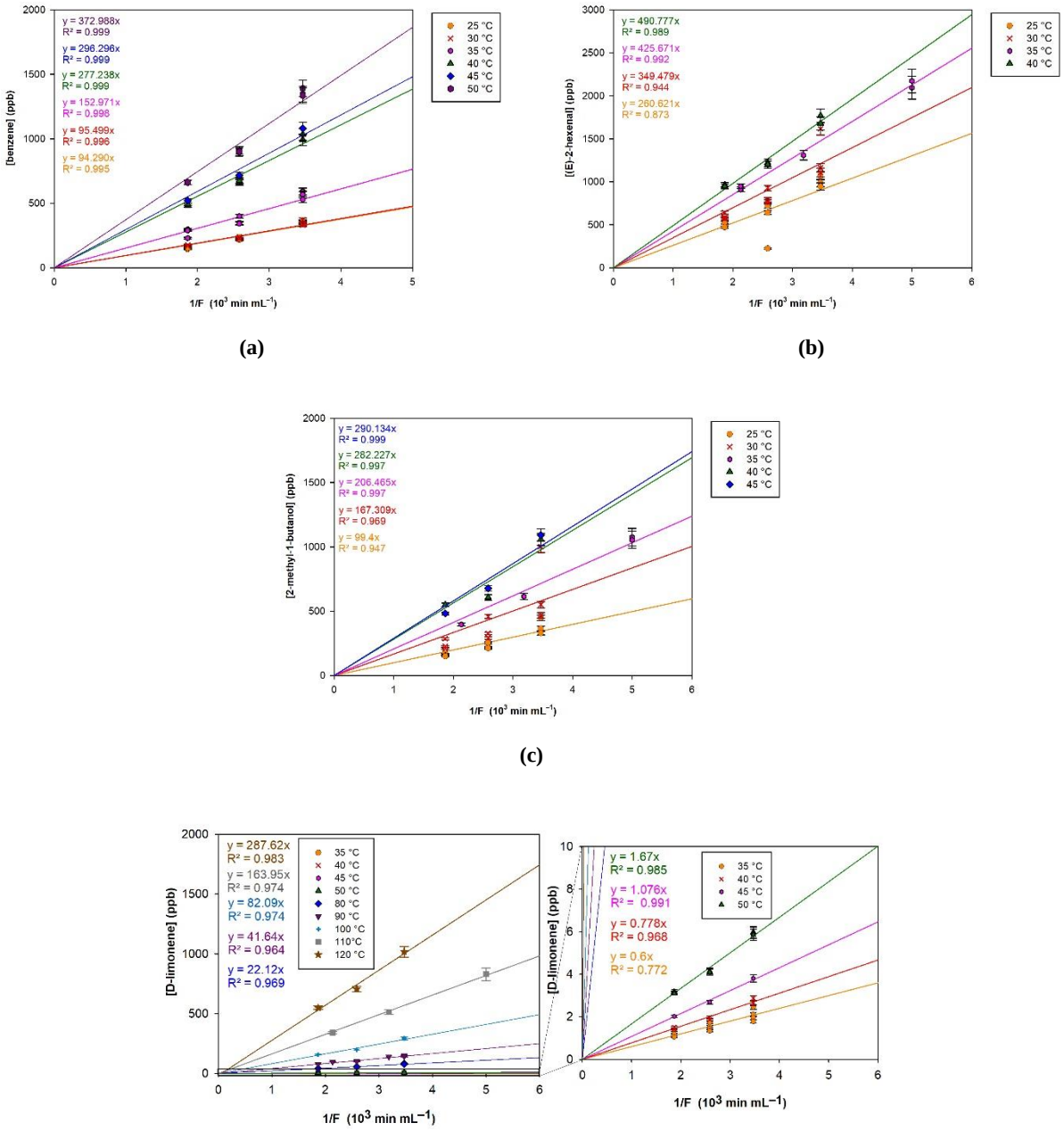

Figure S3. Mean generated concentrations (in ppb) by **a)** benzene, **b)** *(E)*-2-hexenal, **c)** 2-methyl-1-butanol, and **d)** D-limonene (left) permeation tubes measured by online TD-GC-FID method at varying flow rates of 200-, 314-, and 469-mL min^{-1} (at corresponding temperatures of 35, 90, and 110 °C) and flow rates of 288-, 387-, and 536-mL min^{-1} (at corresponding temperatures of 25, 30, 40, 45, 50, 80, 100, and 120 °C, rounded values for clarity), respectively. Inset of the data between 35 and 50 °C is enlarged in (d) for D-limonene (right). Linear regression was fitted for each temperature as a function of the inverse of the total applied flow rates according to the rearranged form of Eq. (6): $C_{VOC_i}\ (ppb) = ER_{VOC_i}(T)/(F_T \times \frac{M_{VOC_i}}{24.04 \times 10^3})$. The slope, expressed in units of 10^{-3} ppb mL min^{-1}, is proportional to the emission rate. Vertical error bars correspond to the uncertainty calculated from the propagated error of the combined MFC1, MFC2, and MFC3 flow rates.

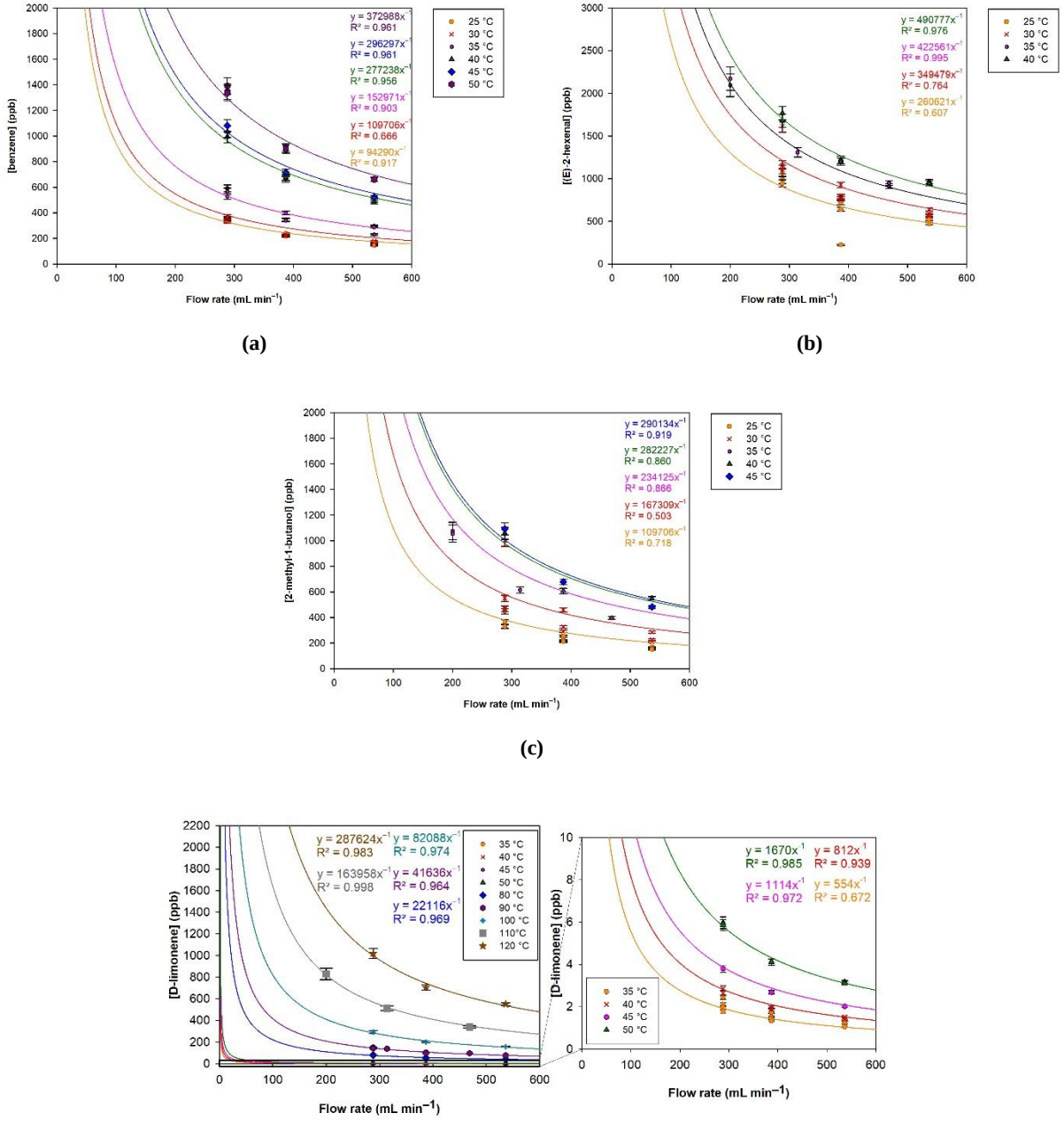

Figure S4. Mean generated concentrations (in ppb) of **a)** benzene, **b)** *(E)*-2-hexenal, **c)** 2-methyl-1-butanol, and **d)** D-limonene (left) measured by online TD-GC-FID method at varying flow rates of 200-, 314-, and 469-mL min^{-1} (at corresponding temperatures of 35, 90, and 110 °C) and flow rates of 288-, 387-, and 536-mL min^{-1} (at corresponding temperatures of 25, 30, 40, 45, 50, 80, 100, and 120 °C, rounded values for clarity), respectively. Inset of the data between 35 and 50 °C is enlarged in (d) for D-limonene (right). An inverse first-order plot was fitted for each temperature according to the rearranged form of Eq. (6): $C_{VOC_i}\,(ppb) = ER_{VOC_i}(T)/(F_T \times \frac{M_{VOC_i}}{24.04 \times 10^3})$. The slope, expressed in units of ppb mL min^{-1}, is proportional to the emission rate. Vertical error bars correspond to the uncertainty calculated from the propagated error of the combined MFC1, MFC2, and MFC3 flow rates.

Table S7. Average generated emission rates of *(E)*-2-hexenal **(a)** at the investigated permeation oven temperatures (25, 30, and 40 °C) and total dilution flow rates of MFC1, MFC2, and MFC3 (288.2-, 387.0-, and 536.4-mL min^{-1}); and **(b)** at 35 °C and total dilution flow rates of MFC1, MFC2, and MFC3 (200.0-, 314.0-, and 468.5-mL min^{-1}). This table reports the mean emission rate, relative standard deviation (RSD), and the total number of measurements for each operating condition (n_{total}). The reported n_{total} includes all the measurements acquired over multiple experimental days (intermediate precision).

Flow	**288.2**			**387.0**			**536.4**			
Temperature (°C)	$ER_{(E)\text{-2-hexenal}}$ (ng min^{-1})	RSD	n_{total}	$ER_{(E)\text{-2-hexenal}}$ (ng min^{-1})	RSD	n_{total}	$ER_{(E)\text{-2-hexenal}}$ (ng min^{-1})	RSD	n_{total}	Average ± 2σ (ng min^{-1})
25	1110.2	6.2%	24	1226.0	5.9%	24	1306.3	5.3%	24	1214.2±197.2
30	1382.3	21.5%	24	1447.6	10.6%	24	1581.4	6.32%	24	1470.4±203.0
40	1995.3	3.6%	16	1979.3	1.2%	16	2092.4	1.3%	16	2022.3±122.4

(a)

Flow	**200**			**314.04**			**468.5**			
Temperature (°C)	$ER_{(E)\text{-2-hexenal}}$ (ng min^{-1})	RSD	n_{total}	$ER_{(E)\text{-2-hexenal}}$ (ng min^{-1})	RSD	n_{total}	$ER_{(E)\text{-2-hexenal}}$ (ng min^{-1})	RSD	n_{total}	Average ± 2σ (ng min^{-1})
35	1742.5	2.6%	16	1677.9	1.2%	8	1741.5	3.6%	8	1720.6±74.0

(b)

Table S8. Average generated emission rates of 2-methyl-1-butanol **(a)** at the investigated permeation oven temperatures (25, 30, 40, and 45 °C) and total dilution flow rates of MFC1, MFC2, and MFC3 (288.2-, 387.0-, and 536.4- mL min^{-1}); and **(b)** at 35 °C and total dilution flow rates of MFC1, MFC2, and MFC3 (200.0-, 314.0-, and 468.5- mL min^{-1}). This table reports the mean emission rate, relative standard deviation (RSD), and the total number of measurements for each operating condition (n_{total}). The reported n_{total} includes all the measurements acquired over multiple experimental days (intermediate precision).

Flow	**288.2**			**387.0**			**536.4**			
Temperature (°C)	$ER_{2\text{-methyl-1-butanol}}$ (ng min^{-1})	RSD	n_{total}	$ER_{2\text{-methyl-1-butanol}}$ (ng min^{-1})	RSD	n_{total}	$ER_{2\text{-methyl-1-butanol}}$ (ng min^{-1})	RSD	n_{total}	Average ± 2σ (ng min^{-1})
25	402.7	16.1%	24	323.1	9.5%	24	311.6	6.7%	24	345.8±99.2
30	711.5	42.7%	24	509.9	24.3%	24	472.8	16.6%	24	564.7±256.9
40	1118.1	1.4%	8	861.3	1.9%	8	1079.9	3.6%	8	1019.8±277.1
45	1153.3	1.4%	8	962.3	0.4%	8	949.3	0.3%	8	1021.6±228.4

(a)

Flow	**200.0**			**314.0**			**468.5**			
Temperature (°C)	$ER_{2\text{-methyl-1-butanol}}$ (ng min^{-1})	RSD	n_{total}	$ER_{2\text{-methyl-1-butanol}}$ (ng min^{-1})	RSD	n_{total}	$ER_{2\text{-methyl-1-butanol}}$ (ng min^{-1})	RSD	n_{total}	Average ± 2σ (ng min^{-1})
35	780.9	1.4%	16	707.5	0.9%	8	681.6	0.3%	8	723.3±103.0

(b)

Table S9. Average generated emission rates of D-limonene **(a)** at the investigated permeation oven temperatures (35, 40, 45, 50, 80, 90, 100, and 120 °C) and total dilution flow rates of MFC1, MFC2, and MFC3 (288.2-, 387.0-, and 536.4- mL min^{-1}); and **(b)** at 90 and 110 °C and total dilution flow rates of MFC1, MFC2, and MFC3 (200.0-, 314.0-, and 468.5- mL min^{-1}). The table reports the mean emission rate, relative standard deviation (RSD), and the total number of measurements for each operating condition (n_{total}). The reported n_{total} includes all the measurements acquired over multiple experimental days (intermediate precision).

Flow	**288.2**			**387.0**			**536.4**			
Temperature (°C)	$ER_{D\text{-}limonene}$ (ng min^{-1})	RSD	n_{total}	$ER_{D\text{-}limonene}$ (ng min^{-1})	RSD	n_{total}	$ER_{D\text{-}limonene}$ (ng min^{-1})	RSD	n_{total}	Average ± 2σ (ng min^{-1})
35	3.38	13.94%	32	3.24	11.31%	32	3.64	12.61%	24	3.4±0.4
40	4.32	5.51%	16	4.37	3.45%	16	5.24	5.56%	16	4.6±1.0
45	6.21	1.12%	8	5.89	1.32%	8	6.14	1.12%	8	6.1±0.3
50	9.68	1.07%	24	9.03	0.70%	24	9.54	1.33%	24	9.4±0.7
80	129.1	4.10%	24	118.9	2.52%	24	124.8	2.96%	24	124.3±10.2
90	238.3	3.04%	24	221.7	2.25%	24	233.9	1.61%	24	231.3±17.2
100	478.0	1.49%	8	436.2	2.05%	8	476.8	0.95%	8	463.7±47.6
120	1662.9	2.03%	8	1548.6	1.99%	8	1672.5	1.82%	8	1628.0±137.8

(a)

Flow	**200**			**314.04**			**468.5**			
Temperature (°C)	$ER_{D\text{-}limonene}$ (ng min^{-1})	RSD	n_{total}	$ER_{D\text{-}limonene}$ (ng min^{-1})	RSD	n_{total}	$ER_{D\text{-}limonene}$ (ng min^{-1})	RSD	n_{total}	Average ± 2σ (ng min^{-1})
90	n.a.	n.a.	n.a.	247.5	2.12%	8	259.1	1.28%	8	253.3±16.4
110	940.2	1.80%	8	912.4	1.55%	8	906.0	2.14%	8	919.5±36.4

(b)

Equation S1. Relative uncertainties on the 3 MFCs flow rate measurements.

$$\frac{\Delta F_1}{F_1} = (0.34\% \times F_{RS1}) + (1\% \times F_{FS1})$$

$$\frac{\Delta F_2}{F_2} = (0.26\% \times F_{RS2}) + (1\% \times F_{FS2})$$

$$\frac{\Delta F_3}{F_3} = (0.5\% \times F_{RS3}) + (1\% \times F_{FS3})$$

where $\frac{\Delta F_1}{F_1}$, $\frac{\Delta F_2}{F_2}$ and $\frac{\Delta F_3}{F_3}$ are the relative uncertainties on the 3 MFCs flow rates, F_{RS1}, F_{RS2}, and F_{RS3} are the flow rates of MFC1, MFC2, and MFC3, respectively at reading-scale of the corresponding MFC, F_{FS1}, F_{FS1}, and F_{FS3} are the flow rates of MFC1, MFC2, and MFC3, respectively, at full-scale of the corresponding MFC.

Table S10. Arrhenius regression parameter values for the investigated permeation tubes, including the fitted slope, apparent activation energies, and pre-exponential Arrhenius factors.

Compound	B	E_a (kJ mol^{-1})	A''
Benzene	–6001±1608	49.9±13.4	$(1.37\times10^{11})\pm(1.71\times10^{2})$
***(E)*-2-hexenal**	–3124±196	25.9±1.7	$(4.36\times10^{7})\pm(1.89)$
2-methyl-1-butanol	–5059±1694	42.1±14.1	$(9.18\times10^{9})\pm(2.4\times10^{2})$
D-limonene	–9225±270	76.7±2.2	$(2.58\times10^{13})\pm(2.18)$

Table S11. Range of extrapolated generated concentrations (in ppb) calculated according to the linear regression plots according to their investigated temperature ranges and compounds (benzene, *(E)*-2-hexenal, 2-methyl-1-butanol, and D-limonene).

Temperature (°C)	Benzene	*(E)*-2-hexenal	2-methyl-1-butanol	D-limonene
25	78.3–680.9	263.2–2287.9	83.4–725.4	n.a.
30	80.3–697.7	318.7–2770.6	136.3–1184.6	n.a.
35	125.7–1092.8	373.0–3242.1	174.6–1517.4	0.5–4.6
40	224.2–1948.9	438.4–3810.6	246.1–2139.4	0.7–6.2
45	233.0–2025.3	n.a.	246.5–2143.1	0.9–8.3
50	293.1–2547.6	n.a.	n.a.	1.5–12.8
80	n.a.	n.a.	n.a.	19.4–168.7
90	n.a.	n.a.	n.a.	37.8–328.9
100	n.a.	n.a.	n.a.	72.4–629.4
110	n.a.	n.a.	n.a.	143.6–1248.2
120	n.a.	n.a.	n.a.	254.2–2209.9

Table S12. Non-exhaustive overview of permeation devices for various VOCs within the atmospheric context reported in the literature, including their calibration methods, material and membrane characteristics, emission rates, and generated concentrations. Geometric dimensions are reported in terms of length, internal diameter (ID), and thickness (Ø). Alternative dimensions are described in the table footnotes.

Calibration method	Target compound	Amount of target compound	Material for generation (geometric dimensions)	Temperature range (° C)	Flow rate (matrix gas) (mL min^{-1})	Range of emission rates (ng min^{-1})	Generated concentrations (ppb)	Reference
Conventional periodic gravimetry	21 compounds[a] (≥95 %)	n.a.[b]	FEP tubing, DuPont (1.57–4.76 mm ID, δ 0.305–0.762 mm)	13.8–29.1 (single-point measurement at 20, 25, 31, and 93 ° C)	n.a.[b]	6.4 (butane)–2,290 (NO_2)	n.a.[b]	O'Keeffe and Ortman (1966)
Conventional periodic gravimetry	SO_2, H_2S, CF_3CH, CS_2	n.a.[b]	FEP tubing, DuPont (L[c] 2.3–10.3 cm, 4.65 and 12.3 mm ID, δ 0.508 and 0.762 mm)	20.3[d]	100–100,000 (dry clean air)	183 (H_2S)–1,279 (CS_2)	1–10,000	Stevens et al. (1969)
Conventional periodic gravimetry	Vinyl chloride	n.a.[b]	FEP Teflon (n.a.)	30[d]	100 (factory compressed air)	6,147–7,557	50–1,030[e]	Bankovich and Modrell (1976)
Conventional periodic gravimetry	18 halocarbons[f]	n.a.[b]	FEP Teflon (L[c] 8.13 cm, 3.175–4.826 mm ID, δ 0.762–3.175 mm)	31[d]	15 (prepurified helium) + 5,000 (dilution)	64.8–14,160	3–130	Singh et al. (1977)

Conventional periodic gravimetry	12 halocarbons[g]	n.a.[b]	FEP tubing, DuPont (δ 0.3, 0.9, and 3 mm)	25[d]	10–150 (high-purity N_2)	n.a.[b]	0–0.06 (CH_2Cl_2)	Crescentini et al., (1981)
Conventional periodic gravimetry	NO_2, SO_2, H_2S, COS, CS_2, DMS	200–300 mg pure gas	PTFE plug on top of a stainless-steel cylinder (L[c] 7 cm)	25–60	Varying up to 50,000 (dry clean air)	10–1,000	0.001<[gas]<1	Beltz et al. (1986)
Conventional periodic gravimetry	BTEX	n.a.[b]	PTFE (L 2–10 cm, 4.826 mm ID, δ 0.762 mm) FEP tubings (L[c] 0.5–5 cm, 3.236 mm ID, δ 0.762 mm)	10–40	0–200 (pure zero-air) + 0–30,000 (dilution)	100–400 (PTFE) ~ 20 (FEP)	1–100 (PTFE) ~ 0.1 (FEP)	Pérez Ballesta et al. (1999)
Thermogravimetry	Benzene	n.a.[b]	Teflon (L 2 cm, 1.5 mm ID, δ 0.85 mm)	31[d]	8.3 (N_2)	20–22	n.a.[b]	Maria et al. (2002)
Thermogravimetry	BTEX	80% of PT internal volume	PTFE Teflon (L[c] 2, 3, and 4 cm, 1.6 and 4.8 mm ID, δ 0.8 mm)	31–51	8.3 (zero-air)	25.76–349.68 (at 31 °C)	n.a.[b]	Tumbiolo et al. (2005)
Magnetic-suspension gravimetry	SO_2 diluted in N_2	n.a.[b]	n.a.[b]	n.a.[b]	50 (N_2) + 500–2,000 (dilution)	≈ 744–774	< 200	Knopf (2001)

Magnetic-suspension gravimetry	SF_6, HFC-125, HFO-1234yf, HCFC-132b, CFC-13	n.a.[b]	Polymeric membrane sealing a stainless steel reservoir (n.a.)	45[d]	5,000 (synthetic air) + 5,000 (dilution)	88.5 (HFO-1234yf)–1654.77 (SF_6)	0.00089 (HFO-1234yf)–0.04182 (HFC-125)	Guillevic et al. (2018)
Magnetic-suspension gravimetry	NH_3 (99.98 %)	n.a.[b]	Polymeric membrane (PTFE or FEP) (n.a.)	30[d]	100 (purified dry synthetic air) + 2-stage dilution (2 × 10,000)	474.6	1–400	Macé et al. (2022)
Offline sampling followed by DNPH-HPLC/UV	CH_3CHO (> 99 %)	2.65 mL	LPDE[h] tubing (L[c] 10 cm, 6 mm ID, δ 1 mm)	10–30	200 (N_2 and compressed air)	2403 (10 °C, N_2)–18349 (30 °C, N_2)	n.a.[b]	Aoyagi et al. (2017)
Offline sampling followed by DNPH-HPLC/UV	HCHO	Low-emission PT: paraformaldehyde High-emission PT: 99.7 mg paraformaldehyde	Low-emission PT: n.a. High-emission PT: PDMS in a ¼” stainless steel nut (9.7 mm D[i], 6.44 mm ES[j], δ 1.5 mm)	Low-emission PT: 50–65 High-emission PT:45–70	Low-emission PT: 30–100 High-emission PT: 30 (ultra-high-purity N_2)	Low-emission PT: 3.09 (50 °C)–14.09 (65 °C) High-emission PT: 178 (45 °C)–1484 (70 °C)	Low-emission PT: 6.8 (35 °C)–378 (65 °C) High-emission PT: 4,836 (45 °C)–40,275 (70 °C)	Grandjean et al. (2024)

Offline sampling followed by DNPH-HPLC/UV	C_3H_6O (99.5 %)	0.5 mL	FEP tubing (L_{eff}[k] ~ 0.1 cm, 3.6 mm ID, δ 1.2 mm)	5–15	200–20,000 (ultra-high-purity N_2)	0.297 (5 °C)–0.677 (15 °C)	0.0086–0.861	Aoyagi et al. (2025)
Offline sampling followed by TD-GC-FID	BTX	n.a.[b]	TFE Teflon (L[c] 14.9–21.8 cm, 9.8 D[i])	30[d]	20–1,200 (ultra-high-purity N_2)	582–767 (benzene) 475–731 (toluene) 148–235 (m-xylene)	200–9090 (benzene) 160–6310 (toluene) 43–1620 (m-xylene)	Susaya et al. (2011)
Offline sampling followed by TD-GC-FID	BTX	n.a.[b]	TFE Teflon (L[c] 14.9–21.8 cm, 9.8 D[i])	30–100	400 and 800 (ultra-high-purity N_2)	624–88,265 (benzene) 485–60,670 (toluene) 188–20,217 (m-xylene)	250–72,700 (benzene) 160–40,300 (toluene) 52–11,000 (m-xylene)	Susaya et al. (2012)
Offline sampling followed by TD-GC-FID	BTEX	n.a.[b]	Polymeric membrane (L[c] 14.9–21.8 cm, 9.8 D[i])	25[d]	50–800 (ultra-high-purity N_2)	398–1,779 (benzene) 338–2,429 (toluene) 44.9–457 (ethylbenzene)	0.69–2.49 (benzene) 0.81–1.8 (toluene) 0.11–0.21 (ethylbenzene)	Kim et al. (2012)

						94.7–1,526 (m-xylene)	0.29–0.44 (m-xylene)	
UV optical absorption	HNO_3 and NH_3	n.a.[b]	HNO_3: FEP Teflon tubing (L^c 6–10 cm, 4.7 and 6.4 mm OD[l]) NH_3: Teflon end caps (L^c 8 cm, 7.4mm OD[l])	25–45	10–50 (dry N_2)	13–150	300–800 (HNO_3) 700 (NH_3)	Neuman et al. (2003)
On-line GC-FID	C_2H_5OH	n.a.[b]	2 silicone-based polymeric membrane: wafer type (4.5 mm D^i, δ 1.5 mm)and EL type (L_{eff}^k 1 cm, 4.5 mm D, δ 1.5 mm)	18–28	50 (N_2) + 150 (dilution)	3,150 (wafer type, 20 °C) 31,550 (EL type, 20°C)	100–500,000	Neri et al. (2006)
On-line TD-GC-FID	Benzene (>99 %) D-limonene (97 %)	1 mL	PTFE tubing (L_{eff}^k 5.5 cm, 4.35 mm ID, δ 1 mm)	25–50 35–120	62 + 68 (dry zero-air) + 0–1000 (dilution)	287.6–1,076.1 3.4–1,628	149.9–661.6 1.2–550.2	This work

	(E)-2-hexenal (98 %) 2-methyl-1-butanol (≥99 %)	1–1.2 mL	PDMS and PTFE enclosed in a 1/8” nut on a stainless-steel reservoir (L_{eff}[k] 6.2 cm, 3.27 mm ID, PDMS δ 2 mm, PTFE δ 2 mm)	25–40 25–45	62 + 68 (dry zero-air) + 0–1000 (dilution)	1,214.2–2,022.3 345.8–1,021.6	495.8–955.5 158.4–549.1	

[a] Propane, butane, SO_2, NO_2, methane, acetylene, CF_3Br, CHF_2Cl, CO_2, ethylene oxide, $CF_3CHClBr$, $CHFCHCH_3$, trans-$CH_3CH{=}CHCH_3$, perfluorodimethylcyclobutane, *n*-C_5H_{12}, benzene, C_6F_6, CF_2I_2, *n*-C_6H_{14}, CH_3CH_2I, H_2S. [b] Not available. [c] total length. [d] Calibration at one operating temperature. [e] for B-900 permeation tube, 6,308 ng min^{-1} emission rate. [f] Methyl chloride, dichloromethane (methylene chloride), chloroform, trichlorofluoromethane (Freon-11), methyl bromide, methyl iodide, phosgene, ethyl chloride, vinyl chloride, 1,2-dichloroethane (ethylene dichloride), trichloroethylene, dichlorotetrafluoroethane (Freon-114), trichlorotrifluoroethane (Freon-113), tetrachloroethylene (perchloroethylene), carbon tetrachloride, 1,1,1-trichloroethane (methyl chloroform), 1,2-dibromoethane (ethylene dibromide), dichlorodifluoromethane (Freon-12). [g] Freon-11, Freon-12, Freon-21, Freon-113, carbon tetrachloride, methyl chloroform (1,1,1-trichloroethane), tetrachloroethylene (perchloroethylene), trichloroethylene, chloroform, dichloromethane (methylene chloride), 1,2-dichloroethane (ethylene dichloride), vinyl chloride. [h] Low-density polyethylene. [i] Diameter. [j] Effective exchange surface. [k] Effective length. [l] Outer diameter.

Table S13. Calculated apparent permeability coefficients *Pr* (*T*) (membrane intrinsic property incorporating both diffusion and solubility effects) for the benzene–PTFE system and D-limonene–PTFE system, determined from experimental emission rates over the temperature range of 35–50 °C, along with the benzene-to-D-limonene permeability ratio (*Pr* (*T*) of benzene/*Pr* (*T*) of D-limonene).

Temperature (°C)	Benzene Pr (*T*)	D-limonene Pr (*T*)	Ratio of Pr (*T*)
35	4.13×10^{-12}	3.85×10^{-13}	10.72
40	5.86×10^{-12}	3.98×10^{-13}	14.73
45	4.90×10^{-12}	4.07×10^{-13}	12.02
50	4.99×10^{-12}	4.89×10^{-13}	10.21

Table S14. Calculated apparent permeability coefficients *Pr* (*T*) (membrane intrinsic property incorporating both diffusion and solubility effects) for the *(E)*-2-hexenal–PDMS/PTFE system and 2-methyl-1-butanol–PDMS/PTFE system, determined from experimental emission rates, over the temperature range of 35–50 °C, along the *(E)*-2-hexenal-to-2-methyl-1-butanol permeability ratio (*Pr* (*T*) of *(E)*-2-hexenal/*Pr* (*T*) of 2-methyl-1-butanol).

Temperature (°C)	*(E)*-2-hexenal Pr (*T*)	2-methyl-1-butanol Pr (*T*)	Ratio of Pr (*T*)
25	2.36×10^{-9}	1.68×10^{-10}	14.05
30	2.08×10^{-9}	1.97×10^{-10}	10.58
35	1.80×10^{-9}	1.84×10^{-10}	9.80
40	1.58×10^{-9}	1.91×10^{-10}	8.26